KSTLE International Journal, Vol. 3, No. 2, December 2002, pp. 101-109

The Pumping Characteristics of the Valveless Peristaltic Micropump by the Variation of Design Parameters

In-Bae Chang†, Dae-Seob Park*, Byeng-Hee Kim and Heon-Young Kim

Department of Mechanical Engineering and Mechatronics, Kangwon National University
**Graduate School, Department of Mechanical Engineering and Mechatronics, Kangwon National University*

Abstract: This paper presents the fabrication and performance inspection of a peristaltic micropump by flow simulation. The valve-less micropump using the diffuser/nozzle is consists of base plate, mid plate, top plate and connection tubes for inlet and outlet. In detail, the base plate is composed of two diffuser nozzles and three chambers, the mid plate consists of a glass diaphragm for the volumetric change of the pumping chamber. The inlet and outlet tubes are connected at the top plate and the actuator for pressing the diaphragm is located beneath the top plate. The micropump is fabricated on the silicon wafer by DRIE (Deep Reactive Ion Etching) process. The pumping performances are tested by the pneumatic test rig and compared with the simulated results for various dimensions of diffuser nozzles. The pumping characteristics of the micropump by the volumetric change at the pumping chamber is modeled and simulated by the commercial software of FLOW-3D. The simulated results shows that reverse flow is the inherent phenomena in the diffuser nozzle type micropump, but it can be reduced at the dual pumping chamber model.

Key words: Peristaltic micropump, diffuser, nozzle, DRIE (Deep Reactive Ion Etching), flow rate, reverse flow

Introduction

The MEMS (Micro Electro Mechanical System) technologies are broadly applied such as micro structures, sensors, actuators, micro robots and etc. The major interests in the field of MEMS are mechanical and/ or electronic systems, whose major dimensions are few millimeters to few micrometers. Around the 1970s, the pressure sensor was produced by the process of bulk micromachining with the silicon wafer and it was the beginning of the micro machining technologies. Now days, the micromachining technologies gives synergy effects by the connection with IT (Information Technology) and BT (Bio Technology). Especially, in the field of medical products, lots of efforts are performed to apply the micropump for drug delivery, genetic analysis and etc. For medical usage, the flow rate should be controlled, the deterioration of the fluidic material by the environmental effects, such as heat, should be avoided in the pumping procedure and back flow should be avoided also [1].

In order to transport the sample or reagents via microchannel or in order to get the optimal process flow to mix, react, separate, dilute and refine the fluidic material, it needs pump and valve elements. Generally, the types of pump sand valves can be divided into active and passive style. The forward and reverse flows are controlled by changing the geometrical shapes of flow channel, in the passive style pump and/or valve. But in the active style, the flow is controlled by the external forces such as electrical field, magnetic field and current that various researches for the microactuators such as static electricity, piezo, thermocouple, shape memory alloy, and etc are vigorously undergoing [2]. Among them, the first valveless micropump using the diffuser nozzle is developed at 1993 [3,4]. The cross section of the diffuser is gradually increased but the cross section of the nozzle is gradually decreased. In the diffuser nozzle style micropumps, the diffuser element does not have any moving parts that it is originally possible to eliminate the fatigue problems of the moving elements which is the most serious problem in the micro machines and it is also possible to reduce the clogging problem. The fluid is transported by the volumetric change at the pumping chamber of the diffuser nozzle style micropump that it is possible to call them volumetric pump and it delivers the fluid periodically, similar to other volumetric pumps.

Generally, the micromachining technology deals with the silicon wafer because the machinability of the silicon material is very consistent but there is a lot of doubts in terms of biological, chemical, electrical and thermal stability that the pyrex glass material is preferred for the substrate material of the micropump because it is very stable for the biological and chemical environments. Therefore, the ultimate purpose of this research is the development of micropump with pyrex glass material. Prior to the pyrex glass product, the micropumps with various design parameters are manufactured with using the silicon material and its performances are tested experimentally and simulated theoretically in order to verify the performances of the diffuser nozzle style micropumps.

In this paper, the diffuser nozzle style valveless micropumps

†Corresponding author; Tel: 82-33-250-6375, Fax: 82-33-257-4190
E-mail: meinster@hanmir.com

are designed for pumping the nano liter scale and manufactured with using the silicon wafer. The test rig with pneumatic actuators is developed to measure the pumping performances of the pumps and the experimental results are compared with the simulated results. Furthermore, in order to reduce the back flow phenomena in the diffuser nozzle style micropumps, the models of dual pumping chamber is simulated also.

The operating principles and structures of the micropump

Fig. 1 shows the basic structures of the diffuser-nozzle style micropump which is used in this paper. The micropump is composed of base, middle and top plate and they are bonded together. The outside dimensions of the micropump is $15 \times 7 \times 1.7$ mm. The size of the base plate is $15 \times 7 \times 0.5$ mm and made of silicon. As shown in Fig. 1 (a), there are three chambers and two nozzles are engraved on the base plate and they are inlet chamber, pumping chamber, outlet chamber, inlet diffuser and outlet nozzle, respectively. The depths of all elements are 80 μm and the inlet and outlet chambers are connected with pumping chamber by diffuser-nozzles. The void volume of inlet and outlet chamber is identically 180 μl and the void volume of the pumping chamber is 1040 μl the inlet width of the diffuser-nozzle is 80 μm and the outlet width is 260 μm. The length of the nozzle is 1080 μm and the opening angle should be decided with considering the viscous friction at the nozzle boundary. The diffuser-nozzles and the chambers are machined by etching process on the base plate in the perpendicular direction and the opening angle of the diffuser is 9.8°. The size of middle plate is $15 \times 7 \times 0.2$ mm and made of 7740 pyrex glass. The Young's modulus of the pyrex glass is 7.2 GPa and the thermal expansion ratio is 3.6×10^{-6}/°K. The thru holes of 100 μm diameter for inlet and outlet are machined on the middle plate and they are connected to the tubes at the top plate. The top plate is made of acryl and the silicon rubber is used for sealing between the top and middle plate. The friction ratio of the diffuser and nozzle is different during the volumetric reduction and expansion of the pumping chamber that the medium can be pumped. The diffuser and nozzle are generally used together at the valveless micropump. If some air is remained in the micropump during the pumping period, the air absorbs the pumping pressure and blocking the flow that the remaining air should be absolutely removed. In order to removing the air in the micropump, the priming process for filling the liquid media inside of the void region of the micropump should be performed. In general priming process, feeding the CO_2 gas into the void for few minutes before pumping the liquid media because the CO_2 gas can be totally melted into the water that it is possible to remove the gas inside of the micropump. But the process needs many uncomfortable equipments and time that the methyl alcohol is used instead of CO_2 gas in this paper [4,5]. The Fig. 1(b) and (c) shows the two types of the base plate. The six models are designed and tested in this paper that five of them have the rectangular shape chamber as shown in Fig. 1(b) and one of them has circular shape as shown in Fig. 1(c).

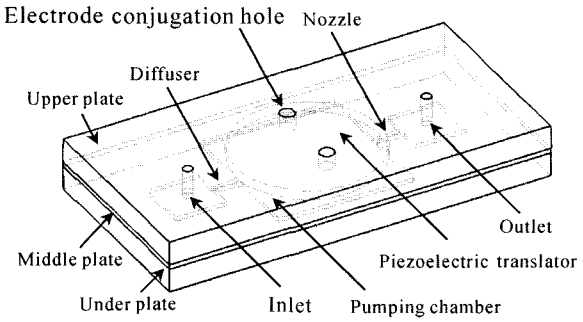

(a) Projection of the micropump

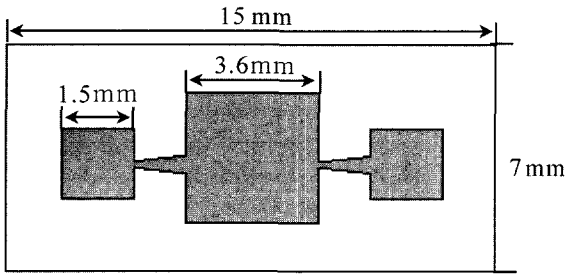

(b) Top view of the square chamber in under plate

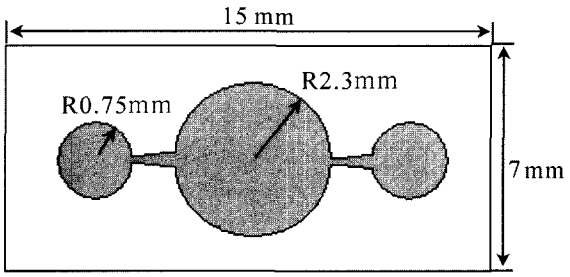

(c) Top view of the circle chamber in under plate

Fig. 1. Structure of the micropump.

The manufacturing process of micropump

The micropump is composed of baseplate, middle plate and tep plate, in this paper. The shapes of flow channel on the base plate are most important factor for the pumping performances of the micropump. In order to ensure the geometrical accuracy of the micropump, the semiconductor production process is adopted for the production of base plate [6-9].

The shapes of micropumps are designed by using the commercial CAD tool and the lithographic mask is fabricated for the base plate. Six types of micropumps are designed for the chamber shapes and nozzle dimension variations on the lithographic mask. Fig. 2 shows the fabrication process of the base plate on the wafer. 0.5 μm~1 μm thickness of photoresist is coated on the oxidated 4 inch silicon wafer and the ultraviolet light is radiated through the mask of the shape of micropump to patterning the shape of micropumps on the photoresist coated 4 inch silicon wafer. The patterns are

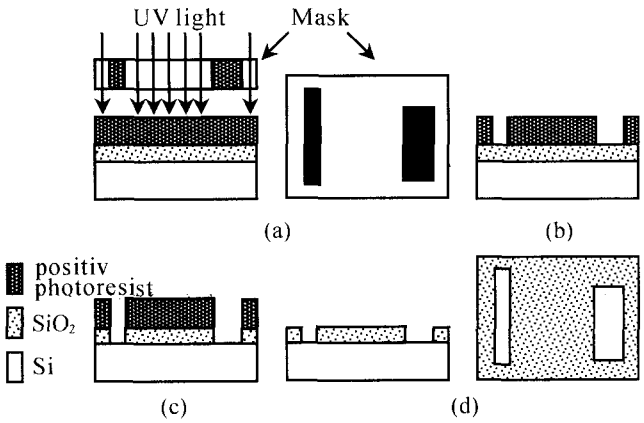

Fig. 2. The schematics of DIRE fabrication process on Silicon wafer.

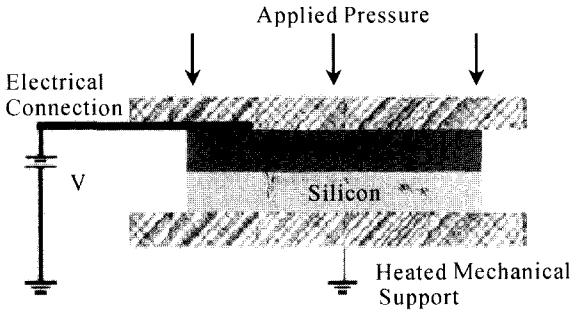

Fig. 3. The basic principle of Anodic bonding process.

macined by the DIRE (Deep Reactive Ion Etching) process. The DIRE process is a dry etching process that the machining time is shorter than the wet etching process, the shape of etched cross-sectin is anisotropic and the precision etching is possible. Furthermore, the smaller size micropump can be fabricated by using the DIRE process. The inlet and outlet holes are machined by using the Excimer laser (KrF) on the middle plate which is made of 0.2 mm thickness pyrex glass. After aligning the machined base and middle plate, the silicon/glass bonding procedure is performed by using the anodic bonding technique. The anodic bonding technique is mainly adapted on glass to glass bonding which contains the silicon and alkali metal and the technique rely upon the mobility of charges between the boards [10,11]. For example, the pyrex 7740 glass board is frequently used for this purpose and it contains about 4.2% of Na_2O. The glass board and the silicon board is attached face to face as shown in Fig. 3 and the Na^+ ions are generated in the glass and moved to the negative electrode when the intensive negative voltage is introduced at the backside of the glass board. As a result, the charged zone is created at the interface between the silicon and glass board and they attract intensively for each other. On this occasion, the mobility of the positive ions are increased proportion to the temperature rise and by the effect of electric field, the oxygen which is migrated from the interface of the glass board joined with silicon to form the layer of SiO_2 to make strong bonding. By using this bonding mechanism between the silicon/glass

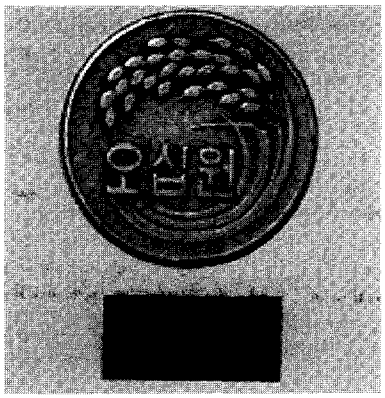

Fig. 4. The size comparison between the micropump and 50 won coin.

material, the micropump can be fabricated with thin film style and it is possible to apply this technique into silicon to silicon bonding and/or glass to glass bonding. The upper plate is made of acryl material for ease of fabrication and visual pumping monitoring. The grooves for actuating the diaphragm, inlet and outlet holes are engraved beneath the top plate and the silicon rubber gasket is used to sealing between the top plats and micropump. Fig. 4 shows the size comparison between the micropump and 50 won coin.

The performance test of the micropumps

The pneumatic actuator with constant air pressure is adapted for the performance test of the micropumps with standardized test scheme. The block diagram of the test rig for the performance test is shown in Fig. 5 (a) and the test system is shown in Fig. 5 (b). The 4 kg/cm^2 of air pressure and 0 kg/cm^2 of vacuum pressure is alternatively applied to the diaphragm region of the micropump in this test system. Therefore, the diaphragm of 0.2 mm thickness pyrex glass at the pumping region is compressed about 640 gram and attracted about 160 gram alternatively. The pumping can be initiated after the priming process because the remaining air disturbs the liquid flow and acts as a damper. In order to overcome this problem, fill the soluble gas such as CO_2 or fill the water in the micropump before initiate the pumping. Various solutions are purposed in the papers [12,13] and it needs more active approach for this problem.

Table 1 shows the 6 pumps for the performance test and their flow rates, respectively. The gray boxes in the table mean the nozzle does not have the round at the inlet region. The flow rates of the micropumps are different each other according to their design parameters and varied from 42.3 nl to 163 nl. The model of PUMP 4 transfers the 0.589 m of water by 3,600 stroke that the pumping capacity of this model is 163 nl/stroke and this capacity is very close to the object value of 150 nl/stroke for this paper. The resultant pumping ratio can be modulated by changing the vibration frequency of the diaphragm on the pumping chamber.

Table 1. The design specifications of the micropumps and their performance test result

	Inlet (μm)			Outlet (μm)			Test result (nl/stroke)
	d_1	L_1	D_1	d_2	L_2	D_2	
Pump1	80	1080	260	80	1080	260	62.5
Pump2	80	1080	260	80	1400	234	44
Pump3	80	1080	260	80	1080	260	73
Pump4	80	1080	260	96	1080	378	163
Pump5	60	1000	228	60	1000	228	42.3
Pump6	Inlet(ϕ1.5), Outlet(ϕ1.5), Pump cavity(ϕ4.6), Circle chamber						21.1

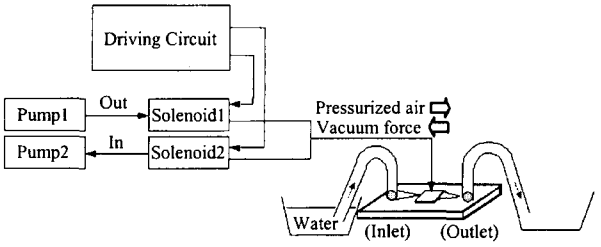

(a) Schematic diagram of the test rig

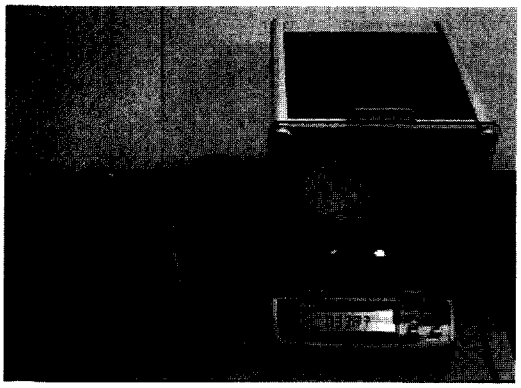

(b) Test rig setup

Fig. 5. The test rig for the performance test of the micropump.

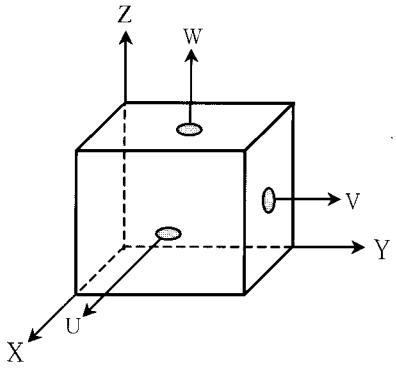

Fig. 6. Control volume.

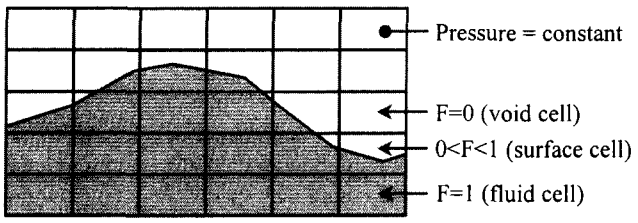

Fig. 7. Volume fraction at the control volume.

The flow analysis of the micropump

In order to explain the flow phenomena and characteristics, the commercial flow analysis software of FLOW-3D is used in this paper. The 6 pump models are designed and simulated according to the design parameters of the diffuser and shape of the chamber and the results are discussed according to the boundary conditions and their flow rates. The main purposes of this analysis are the performance comparisons of the flow characteristics according to the shape variations of the chamber, according to the length variations of the diffuser, according to the existence of the round at the inlet region of the diffuser, and etc.

The theory of flow analysis -governing equation

The total analysis region is divided into small cells as shown in Fig. 6 by using the finite volume method (FVM) and the continuity equation, momentum equation, energy conservation equation, laminar and turbulent flow equation is used to solve the flows in the micropump. The three dimensional free surface can be described by the VOF (volume of fluid) technique as shown in Fig. 7. The free surface is defined by the factor F (volume friction) which indicates the states of filling by fluid in the cell.

The governing equations for the analysis are derived on the basis of Decart coordinate and given as follows.

(1) Continuity equation

$$\frac{\partial}{\partial x}(uA_x) + \frac{\partial}{\partial y}(vA_y) + \frac{\partial}{\partial z}(wA_z) = \frac{RSOR}{\rho} \quad (1)$$

u, v and w designate the velocity of each direction, ρ is the density, RSOR is the source of mass.

(2) momentum equation

the momentum equation describes the Newton's second law that the differential momentum equation for the flow is given as;

$$\frac{\partial u}{\partial t}+\frac{1}{V_f}\left\{uA_x\frac{\partial u}{\partial x}+vA_y\frac{\partial u}{\partial y}+wA_z\frac{\partial u}{\partial z}\right\}=-\frac{1}{\rho}\frac{\partial P}{\partial x}+F_x-\frac{ROSR}{\rho V_f}u$$

$$\frac{\partial v}{\partial t}+\frac{1}{V_f}\left\{uA_x\frac{\partial v}{\partial x}+vA_y\frac{\partial v}{\partial y}+wA_z\frac{\partial v}{\partial z}\right\}=-\frac{1}{\rho}\frac{\partial P}{\partial x}+F_y-\frac{ROSR}{\rho V_f}v \tag{2}$$

$$\frac{\partial w}{\partial t}+\frac{1}{V_f}\left\{uA_x\frac{\partial w}{\partial x}+vA_y\frac{\partial w}{\partial y}+wA_z\frac{\partial w}{\partial z}\right\}=-\frac{1}{\rho}\frac{\partial P}{\partial x}+F_z-\frac{ROSR}{\rho V_f}w$$

compare to the continuity equation, the factor of RSOR designates the acceleration.

(3) energy equation

$$V_f\frac{\partial}{\partial t}(\rho I)+\frac{\partial}{\partial x}(\rho IvA_x)+R\frac{\partial}{\partial y}(\rho IwA_y)+\frac{\partial}{\partial z}(\rho IwA_z)+\varepsilon\frac{\rho IuA_x}{x}$$

$$=-p\left\{\frac{\partial uA_x}{\partial x}+R\frac{\partial vA_y}{\partial y}+\frac{\partial wA_z}{\partial z}+\varepsilon\frac{uA_x}{x}\right\}+RIDIF+TDIF+RISOR \tag{3}$$

the RIDIF is an expansion of turbulent flow, TDIF is a conduction through the solid material and RISOR is a term of energy generation.

(4) volume of fluid equation

$$\frac{\partial F}{\partial t}+\left\{\frac{\partial}{\partial x}(FuA_x)+\frac{\partial}{\partial y}(FvA_y)+\frac{\partial}{\partial z}(FuA_z)\right\}=FDIF+FSOR \tag{4}$$

here, the FDIF is a diffusion of fluid fraction and FSOR is a source of fluid.

Design parameters and boundary conditions

The basic design models are classified by the shapes of the chamber such as circular and rectangular and the detail models are derived by changing the design parameters for the diffuser. Fig. 8 shows the base plate of the micropump which have the rectangular shape chambers and the diffuser is magnified in order to show the round shape.

The design parameters are the inlet width of the diffuser (d), outlet width of the diffuser (D), the length of the diffuser (L) and the existence of the round at the inlet region is an important design parameter. The schematic shapes of the diffuser are shown in the Fig. 9. In order to find out the influence of the design parameters of the diffuser into the pumping flow rates, the simulation is carried out according to the 6 pump models. The design parameters of the micropumps are the same as the experimented models and given in the Table 1.

The boundary conditions for the simulation are given in the Fig. 10. Theoretically, the optimal actuating frequencies for the moving obstacle is around 1~10 Hz [14] and 4 Hz is selected in this paper. The amplitude of the actuator is selected to 40 μm which is halt of the chamber depth and the material property of the fluid is selected for the water. The flow at the outlet should be continuous for the ideal micropump, but it is inevitable to protect the reverse flow. Therefore, the flow simulation should be performed before the fabrication of the micropump. Even if the micropump satisfies the specifications of flow rates, the reverse flow may make some serious problems that the simulation should be performed prior to the fabrication [15].

Results and discussions

Discussions for the simulation results

The Fig. 11 shows the variations of the flow velocity at the diffuser and nozzle as the diaphragm of the mid plate goes down by the vibration of the PZT and Fig. 12 shows the variations of the flow for the time at the inlet and outlet respectively that the flow rate at the inlet and outlet are almost constant during compression and retraction period. The variation of the flow rate by the diaphragm vibration is 0.023 mm^3/sec = 0.023 μl/sec. As the elongation of the nozzle length, the viscous friction is increased and the total flow rate is decreased in the model of PUMP 2 than PUMP 1. But the variation of the flow rate at the outlet is smaller and the reverse flow is smaller also that the performance of the PUMP 2 is better than the model of PUMP 1. The variation of the flow rate in the PUMP 2 is 0.015 mm^3/sec.

The model of PUMP 3 is exactly the same as PUMP 1 except for the absence of round at the outlet of the nozzle. The flow rate of the PUMP 1 is 0.023 mm^3/sec and the flow rate of the PUMP 3 is 0.031 mm^3/sec that the more fluid can be pumped in the model of PUMP 3. This is due to the removal of the round at the nozzle region and we can find out the effect of the round at the nozzle to the flow rate. The variation of the flow rate in the PUMP 3 is 0.031 mm^3/sec. In the model of PUMP 4, the dimensions of d_2, D_2 are increased than PUMP 3 but other parameters are the same. But the simulation result shows that much more fluid can be pumped in this model. This

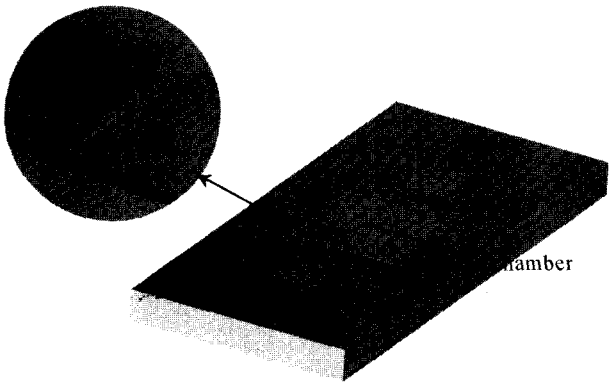

Fig. 8. Square chamber from under plate of micropump.

* $2\theta = 9.8°$
* Depth of chamber = 80μm

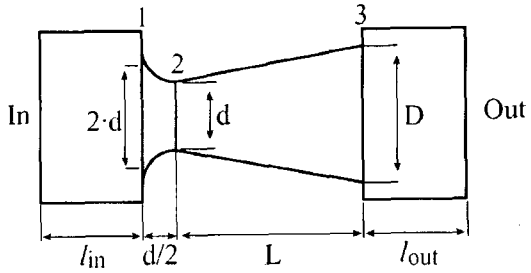

Fig. 9. Geometry of the diffuser.

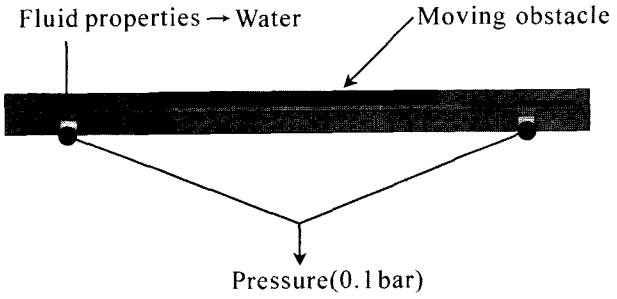

Fig. 10. Boundary conditions of micropump.

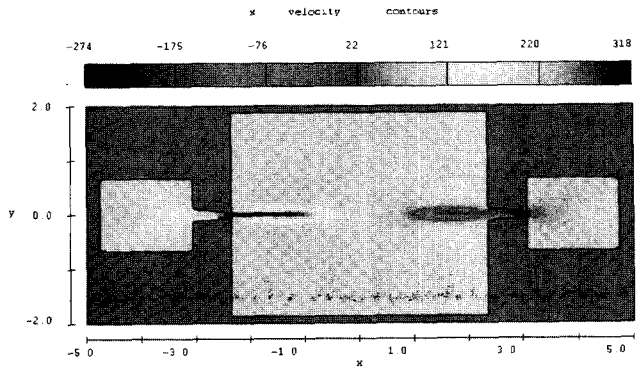

Fig. 11. Velocity changed of fluid at pump1.

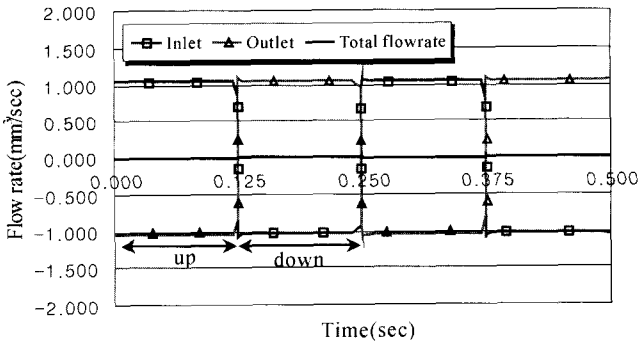

Fig. 12. Flow rate of pump1.

shows that the increase of d_2, D_2 at the nozzle region lead to the increase the flow rate. The highest flow rate is shown in the PUMP 4 but the variation of the flow rate is too much that this model is inferior to others for the purpose of micropump. The variation of the flow rate in the PUMP 4 is 0.044 mm³/sec. The size of d and D at the diffuser and nozzle are decreased at the PUMP 5 than PUMP 1. The cross sectional area of the diffuser and nozzle are decreased that variation of the flow velocity at the PUMP 5 is much more than PUMP 1. The flow of the fluid at the inlet and outlet are almost constant and the variation of the flow is 0.041 mm³/sec. The model of PUMP 6 has the unique design that has the circular chambers. Fig. 14 shows that the velocity of this model is smaller than that of rectangular chambers. And the irregular flow characteristics are arisen by the turbulence during the diaphragm moves down. This phenomenon is harmful for the micropump because it deteriorates the controllability of the micropump. The variation of the flow rate in the PUMP 6 is 0.028 mm³/sec.

The flow rates of the pumps are compared in the Fig. 16 that the PUMP 4 is most and the PUMP 2 is least performances in point of flow rate. But the micropump deals with the nano liter scale flow rate that basically, all the model satisfies the specifications to be a micropump. But in case of medical usage such as drug delivery, the reverse flow may arise a serious problem that the variation of flow rate at the outlet may be an important design parameter. Considering the point of view, the PUMP 2 shows the best performances.

The variations of flow rates according to the variation of the nozzle length (L) are compared with PUMP 1 and PUMP 2 at the Table 1. The flow rate of the PUMP 1 is 0.023 mm³/sec and the PUMP 2 is 0.015 mm³/sec. All the other dimensions including the round shapes at the entrance and exit of the pumps are the same except for the nozzle length that the difference is due to the increase of the viscous friction by the elongation of the nozzle length.

The effect of the roundness at the diffuser and nozzle to the flow rate can be deduced from the result between the PUMP 1 and PUMP 3. The PUMP 3 and PUMP 4 do not have the roundness at the exit of the nozzle and the flow rates are increased compared to the pump 1. The viscous friction at the wall of the nozzle may decrease at the rounded zone that the flow rate may decrease at the model of the PUMP 1 compared to the models of PUMP 3 and PUMP 4.

The effect chamber shape to the flow rate is compared with

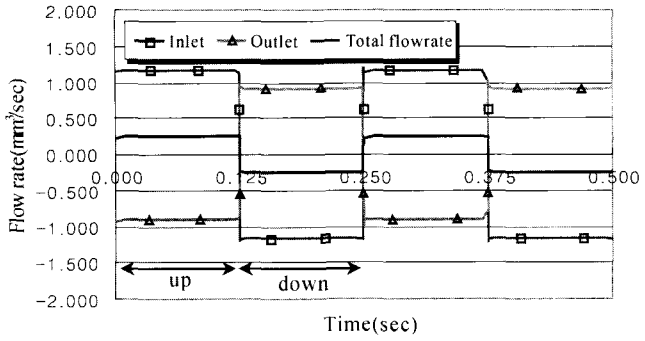

Fig. 13. Flow rate of pump2.

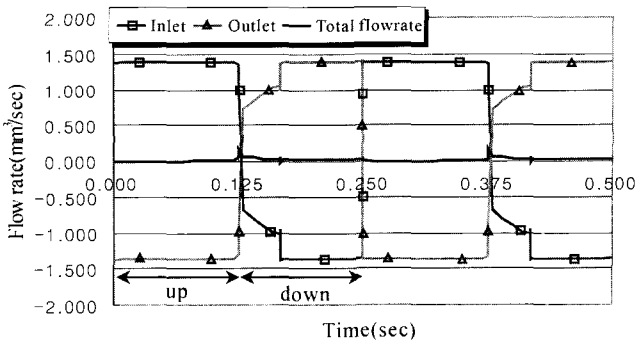

Fig. 15. Flow rate of pump6.

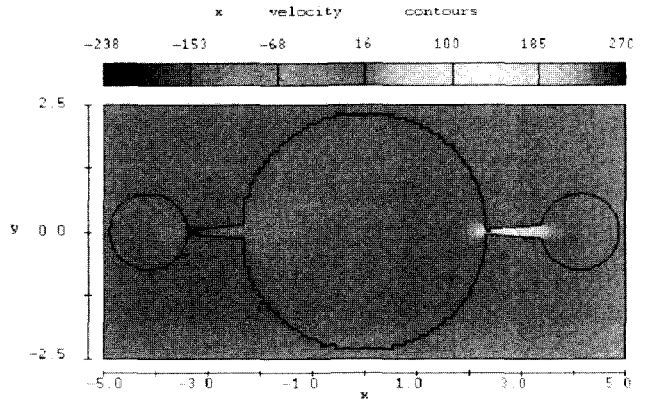

Fig. 14. Velocity changed of fluid at pump6.

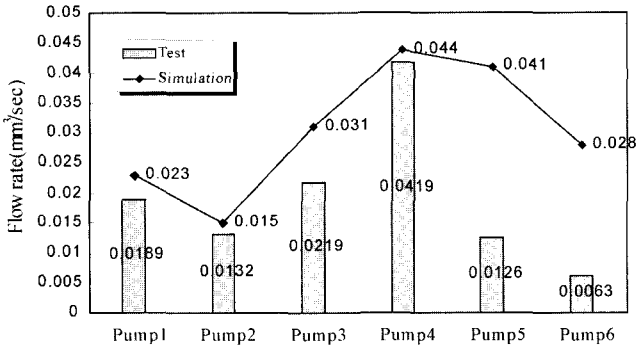

Fig. 16. Flow rate compared with pump models.

the model of PUMP 1 and PUMP 6. It is not possible to assert the difference because the flow rate with the rectangular chamber (PUMP 1) is 0.023 mm³/sec and with the circular chamber is 0.028 mm³/sec that they have very similar result. Consequently, we can deduce that the shapes of the chamber may affect the flow rates but the effect is very small.

The comparison between the simulations and the performance tests

The Fig. 16 compares the simulated results to the test results that the flow rates may have some differences between them but the whole tendencies are very similar between the two results. The models of PUMP 2, 3 and 4 have very similar results but the models of PUMP 1, 5 and 6 have some deviations.

The first cause of the deviations is imperfection of the theoretical model. The modern theory for the turbulent flow can not exactly describe the turbulent phenomena, which happens in the natural field. Therefore, all the parameters should be approximated during the simulation. The second cause is the simplification. The natural conditions are simplified that it is not possible to sufficiently consider the mutual relationship between the model and real system and selectively consider the chief parameters between the enormous parameters of the observing target. The third cause is the limitation of the grid elements. There are limitations for the flow description if the model has complex shapes. It needs to get the rational grid size and aspect ratio for the target model. The fourth cause is the absurd boundary conditions. It is very difficult to get the exact phenomena at the boundary that there are always some deviations between the real flow and theoretical model. The last cause is the inaccurate values of the material properties such as viscosity, thermal conductivity and etc.

The dual pumping chamber model

The micropump modes of the single pumping chamber are simulated for various design parameters that the flow rates are generally satisfiable, but the reverse flow at the outlet is a still unsolved problem. In order to reduce the reverse flow at the outlet, new design model is proposed and simulated. Fig. 17 shows the simulated pump model which has dual pumping chamber and the shape of diffuser, is magnified in order to show the rounded regions. The all parameters of the diffuser angle, length of the nozzle, depth of the chamber, width of the nozzle and roundness are the same as the model of PUMP 1 in the Table 1 except for the number of pumping chamber. In order to find out the reduction of reverse flow at the outlet, the flow rate of dual pumping chamber model is compared with the result of the PUMP 1 model. The whole boundary conditions are the same in the simulation except for the vibration frequency. In the model of dual pumping chamber, the two diaphragms at the pumping region moves in reverse direction. If the two diaphragm moves in same direction, the flow rate may doubled but the reverse flow at the outlet may doubled also that the reverse movement is adopted to reduce

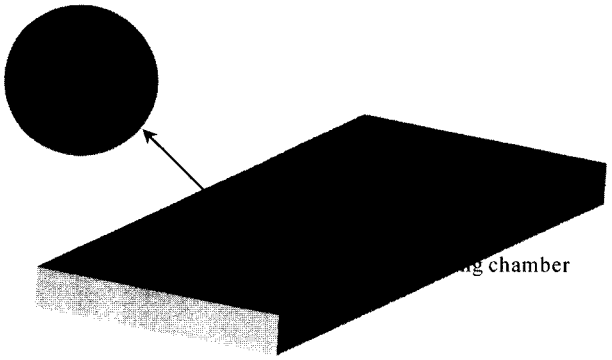

Fig. 17. The picture of double pumping chamber.

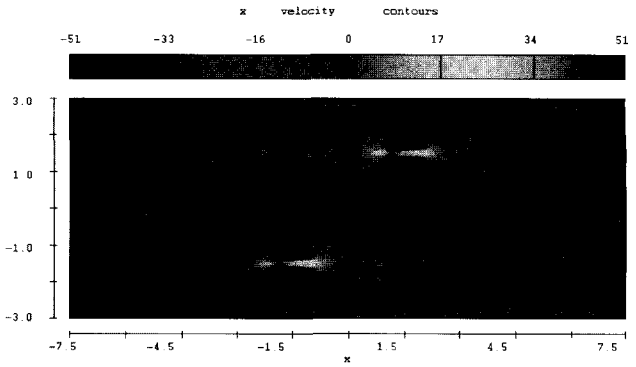

Fig. 18. Velocity changed of fluid at double pumping chamber.

the reverse flow with using the principle of diffuser/nozzle.

The variation of flow velocity according to the diaphragm movement is shown in Fig. 18 and Fig. 19 shows the variation of the flow rate according to the time at the outlet of the micropump. Different from the model of PUMP 1 the direction of the flow at the inlet and outlet are not changed. The flow rate of the dual pumping chamber model is 0.041 mm^3/sec that the flow rate is 1.8 times much than PUMP 1 but the variation of the flow rate is small. Furthermore, the reverse flow at the outlet is –0.023 mm^3/sec in the dual pumping chamber model that comparing the PUMP 1 of –1.039 mm^3/sec, 98% of the reverse flow is reduced. Considering that the forward and reverse flow rate are the most important parameters in the micropump, the dual pumping chamber model is superior to the other models that have single pumping chamber.

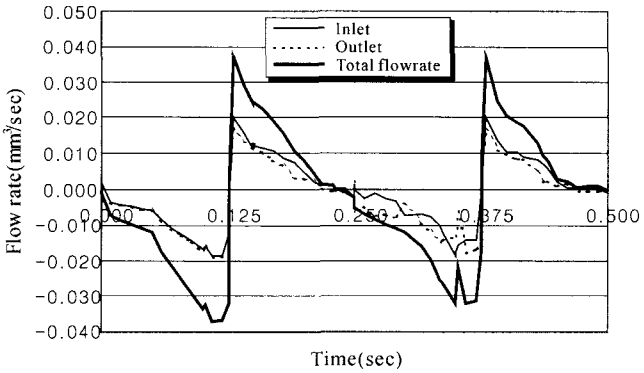

Fig. 19. Flow rate of double pumping chamber.

Conclusion

In this paper, the diffuser-nozzle type micropump which is made of glass and silicon material, are designed, simulated, fabricated and tested prior to the implementation of micropump with pure pyrex glass material. The pumping performances of the micropumps are tested ans compared with the simulated results. In order to reduce the reverse flow, the micropump which has the dual pumping chamber, is proposed and simulated and following results are presented.

1) The DIRE (Deep Reactive Ion Etching) technique is adapted for the machining of micropump on the silicon wafer

2) The anodic bonding technique is adapted for silicon/glass bonding, but it is proved that this technique can be applied to the silicon to silicon and glass to glass bonding.

3) The 6 models of micropump with single pumping chamber are fabricated, tested and compared with the simulated results. The flow rates of the two results are very similar that the simulation model has a good coincidence with the real flow phenomena.

4) In order to reduce the reverse flow at the outlet of the micropump, the dual chamber style micropump is modeled and simulated. The simulated result shows that 1.8 times of the flow rate is increased and 98% of the reverse flow is decreased that the dual chamber style micropump shows a good vision for the practical use.

Acknowledgement

This work is funded by the project of The development of micropump system using the glass piling/bonding technology sponsored by the Korea Ministry of Commerce, Industry and Energy and managed by AnDT Co.

References

1. Y. S. Kim, S. S. Yang, Fabrication and Test of a Micropump by Thin Silicon Plate, Journal of KIEE, Vol. 46, No. 7, pp. 1135-1140, 1997.
2. Korea Institute of Science and Technology Information, The investigation of the trends of new technology on Bio-Chip, 2002.
3. E. Stemme and G. Stemme, A Valve-less Diffuser/Nozzle based Fluid Pump, Sensors and Actuators, vol. A39, pp. 159-167, 1993.
4. E. Stemme and G. Stemme, Valve-Less Fluid Pump, Swedish Patent Appl. No. 9300, 604-607, 1993.
5. P. Gravesen, J. Brandebjerg, and O. S. Jensen, Microfluidics - a review, Journal of Micromechanics and Microengineering, vol. 3, pp. 168-182, 1993.
6. S. Shoji and M. Esashi, Microflow devices and systems, Journal of Micromechanics and Microengineering, vol. 4, pp. 157-171, 1994.
7. M. Elwenspoek, T. S. J. Lammerink, R. Miyake, and J. H. J. Fluitman, Towards integrated microliquid handling systems, Journal of Micromechanics and Microengineerin -g, vol. 4, pp. 227-245, 1994.

8. F. M. White, Fluid Mechanics. New York: McGraw-Hill, 1986.
9. J. G. Smits, Piezoelectric Micropump with Three Valves Working Peristaltically," Sensors and Actuators, vol. A21-A23, pp. 203-206, 1990.
10. R. Zengerle, S. Kluge, M. Richter, and A. Richter, A Bidirectional Silicon Micropump, presented at IEEE 8th International Workshop on Micro Electro Mechanical Systems (MEMS'95), Amsterdam, the Netherlands, Jan. 29 - Feb. 2, 1995.
11. W. Bacher, W. Menz, and W. K. Schomburg, Micropump manufactured by thermoplastic molding, presented at IEEE 7th International Workshop on Micro Electro Mechanical Systems (MEMS'94), Oiso, Japan, January 25-28, 1994.
12. E. H. Klaassen, K. Petersen, J. M. Noworolski, J. Logan, N. I. Maluf, C. Storment, W. McCulley, and G. T. A. Kovacs, Silicon fusion bonding and deep reactive ion etching; a new technology for microstructures, presented at ansducers'95 - Eurosensor IX, Stockholm, Sweden, June 25-29, 1995.
13. T. Gerlach and H. Wurmus, Working principle and performance of the dynamic micropump, Sensor and Actuators, vol. A50, pp. 135-140, 1995.
14. M. Stehr, S. Messner, H. Sandmaier, and R. Zengerle, A New Micropump with Bidirectional Fluid Transport and Selfblocking Effect, presented at IEEE 9th International Workshop on Micro Electro Mechanical Systems (MEMS'96), San Diego, California, USA, February 11-15, 1996.
15. H. T. G. van Lintel, F. C. M. van den Pol, and S. Bouwstra, A piezoelectric micropump based on micromachining in silicon, Sensors and Actuators, vol. 15, pp. 153-167, 1988.
16. Roland Zengerle and Martin Richter, Simulation of Microfluid System, J. Micromech. Microeng, Vol. 4, pp. 192-204, 1994.